Dual function of the NDR-kinase Dbf2 in the regulation of the F-BAR protein Hof1 during cytokinesis

Franz Meitinger[a], Saravanan Palani[a], Birgit Hub[b], and Gislene Pereira[a]
[a]Molecular Biology of Centrosomes and Cilia Unit, DKFZ-ZMBH Alliance, and [b]Department of Tumor Virology, German Cancer Research Center, 69120 Heidelberg, Germany

ABSTRACT **The conserved NDR-kinase Dbf2 plays a critical role in cytokinesis in budding yeast. Among its cytokinesis-related substrates is the F-BAR protein Hof1. Hof1 colocalizes at the cell division site with the septin complex and, as mitotic exit progresses, moves to the actomyosin ring (AMR). Neither the function of Hof1 at the septin complex nor the mechanism by which Hof1 supports AMR constriction is understood. Here we establish that Dbf2 has a dual function in Hof1 regulation. First, we show that the coiled-coil region, which is adjacent to the conserved F-BAR domain, is required for the binding of Hof1 to septins. The Dbf2-dependent phosphorylation of Hof1 at a single serine residue (serine 313) in this region diminishes the recruitment of Hof1 to septins both in vitro and in vivo. Genetic and functional analysis indicates that the binding of Hof1 to septins is important for septin rearrangement and integrity during cytokinesis. Furthermore, Dbf2 phosphorylation of Hof1 at serines 533 and 563 promotes AMR constriction most likely by inhibiting the SH3-domain–dependent interactions of Hof1. Thus our data show that Dbf2 coordinates septin and AMR functions during cytokinesis through the regulation/control of Hof1.**

Monitoring Editor
Doug Kellogg
University of California, Santa Cruz

Received: Aug 20, 2012
Revised: Dec 13, 2012
Accepted: Jan 2, 2013

INTRODUCTION

During cytokinesis one cell physically divides into two daughter cells. As such, cytokinesis must be tightly coordinated with cell cycle progression to ensure proper inheritance of chromosomes and cell organelles (Balasubramanian *et al.*, 2004; Barr and Gruneberg, 2007). In yeast and animal cells, cytokinesis is driven by a contractile actomyosin ring (AMR), which drives membrane ingression, thereby closing the cell division site. In yeast, AMR contraction is accompanied by the formation of a septum, the future cell wall that covers the cell division site. AMR contraction and septum formation are interdependent and tightly coordinated processes (Schmidt *et al.*, 2002). Cyclin-dependent kinase 1 (Cdk1), when complexed with cyclins, is a major regulator of cell cycle progression and negatively regulates cytokinesis (Holt *et al.*, 2009; Meitinger *et al.*, 2012; Palani *et al.*, 2012). In previous studies, other mitotic kinases have been reported to execute essential roles in the coordination of cytokinesis with the cell cycle progression. Among them are the conserved family of NDR-related kinases, which includes LATS1 in human cells and Dbf2 in budding yeast (Frenz *et al.*, 2000; Vallen *et al.*, 2000; Yang *et al.*, 2004; Yoshida and Toh-e, 2001).

Dbf2 is part of a signaling cascade, known as the mitotic exit network (MEN), that activates the mitotic Cdk1-counteracting phosphatase Cdc14 in late anaphase (Bardin and Amon, 2001; Meitinger *et al.*, 2012). The Dbf2-dependent activation of Cdc14 drives cells out of mitosis by reverting the impact of Cdk1 phosphorylation and down-regulating its activity. Of interest, Dbf2 appears at the cell division site after Cdk1 down-regulation and is directly involved in AMR contraction and septum formation (Frenz *et al.*, 2000). Although the mitotic exit function of Dbf2 does not seem to be conserved in higher eukaryotes, LATS1, like Dbf2, has been reported to drive AMR contraction in human cells, indicating functional conservation of the prominent role for this kinase in AMR control in yeast (Meitinger *et al.*, 2011; Yang *et al.*, 2004).

This article was published online ahead of print in MBoC in Press (http://www.molbiolcell.org/cgi/doi/10.1091/mbc.E12-08-0608) on February 27, 2013.

Address correspondence to: Gislene Pereira (g.pereira@dkfz.de).

Abbreviations used: 5-FOA, 5-fluoroorotic acid; AMR, actomyosin ring; CC, coiled coil; Cdk1, cyclin-dependent kinase 1; F-BAR, Fes/CIP4 homology Bin/Amphiphysin/Rvsp; FCH, Fes/CIP4 homology; GST, glutathione *S*-transferase; HA, hemagglutinin; MEN, mitotic exit network; PP2A, protein phosphatase 2A; RLS, ring localization domain; SID, septin interaction domain; TAP, tandem affinity purification.

Dbf2 was reported to recruit the cytokinesis factors Cyk3, Inn1, and Chs2 to the cell division site (Meitinger *et al.*, 2010). Cyk3, Hof1, and Inn1 form a complex that is most likely involved in the activation of the chitin synthase Chs2, the catalytic enzyme that generates the primary septum (Cabib *et al.*, 1993; Nishihama *et al.*, 2009). In addition, Dbf2 was reported to phosphorylate Chs2 (Oh *et al.*, 2012) and the F-BAR protein Hof1 (Meitinger *et al.*, 2011). Dbf2 function on Hof1 depends on a Cdc5 mediated pre-phosphorylation of Hof1, which creates a binding site for Mob1, the regulatory subunit of Dbf2 (Meitinger *et al.*, 2011).

Hof1 appears at the cell division site in S phase, where it colocalizes with the septin collar and is later part of the contractile AMR during the subsequent phase of cytokinesis (Lippincott and Li, 1998; Young *et al.*, 2010). Hof1 overexpression results in an aberrant distribution of septins, which is indicative of a role in the regulation of septin structures (Lippincott and Li, 1998). However, a molecular understanding of the interaction of Hof1 with septins is lacking. Hof1 is a multifunctional protein that possesses an N-terminal F-BAR, a C-terminal SH3 domain, and a ring localization sequence (RLS) that facilitates the association of Hof1 with the AMR (Meitinger *et al.*, 2011). The F-BAR and the RLS are essential for proper AMR contraction, whereas the SH3 domain is dispensable for it (Meitinger *et al.*, 2011). Dbf2 phosphorylates Hof1 at several sites between the F-BAR and SH3 domains (Meitinger *et al.*, 2011). The introduction of phosphomimetic mutations in all of the Dbf2-phosphorylation sites of Hof1 reduced the degree of colocalization of Hof1 with septins during mitosis and supported AMR constriction in the absence of Dbf2 activity (Meitinger *et al.*, 2011). How Dbf2 regulates the septin and AMR bound pools of Hof1 remains to be established.

Here we characterize the molecular function of Dbf2-dependent Hof1 phosphorylation. We find that the interaction between Hof1 and septins relies on a novel coiled-coil region next to the F-BAR domain that is phosphorylated and regulated by Dbf2. Genetic and functional analyses establish that the interaction between Hof1 and septins is required to maintain the integrity of septin structure during mitosis. Furthermore, phosphorylation of Hof1 by Dbf2 at residues next to the SH3 domain promote AMR contraction and septum formation, most likely through inhibition of an SH3-dependent interaction. We therefore propose that Dbf2 influences two independent and separable Hof1 functions during cytokinesis.

RESULTS

A coiled-coil region adjacent to the F-BAR domain mediates the binding of Hof1 to septins

To understand the recruitment of Hof1 to septin rings, we mapped the septin interaction domain of Hof1 using the yeast two-hybrid system (Figure 1A). We found that Hof1 constructs carrying either the F-BAR or SH3 domains but lacking codons 293–355 failed to interact with septins (Figure 1A). This indicated that amino acids 293–355 were critical for Hof1 binding to septins. In line with this, the Hof1 fragment 293–355 localized at the cell division site in a septin-like manner (Figure 1B). Domain prediction analysis identified one coiled-coil domain between amino acids 293 and 333 (Figure 1C). F-BAR domains comprise an FCH domain with an associated coiled-coil region (Aspenstrom, 2009). Three-dimensional (3D) structural modeling revealed that ~280 amino acids at the N-terminus of Hof1 were sufficient to generate the typical banana-shaped F-BAR domain of F-BAR proteins (Figure 1D; Shimada *et al.*, 2007). We therefore concluded that the coiled-coil region that mediates Hof1 binding to septins is not part of the F-BAR domain. Similar results were independently obtained by another group (Oh *et al.*, 2013). We refer to this region between codons 293 and 355 as the Hof1–septin interaction domain (SID).

We previously reported that the F-BAR domain was required for the association of Hof1 with the septin scaffold (Meitinger *et al.*, 2011). This conclusion was based on a Hof1 N-terminal truncation that lacked amino acids 2–299 (Δ2-299). We thus reasoned that either the F-BAR domain contributes to Hof1 septin localization in vivo or the truncation spanning amino acids 2–299 influenced the SID of Hof1. To discriminate between these possibilities, we compared the levels of septin-associated Hof1 truncated forms (Figure 1, E–G). We found that the deletion of either F-BAR domain (Δ2-279) or SID coiled coil (Δ293-333) reduced the association of Hof1 with septins (Figure 1, E–G). The deletion of both F-BAR and coiled-coil regions (Δ2-399) completely abolished Hof1 association with the septin complex (Figure 1, E–G). We therefore concluded that both the F-BAR and SID domains contribute to the association of Hof1 with the septin scaffold in vivo.

Phosphorylation of serine 313 in the SID decreases the binding of Hof1 to septins

We previously reported that phosphorylation of Hof1 by the Dbf2-Mob1 kinase complex leads to the premature release of Hof1 from the septin collar during metaphase (Meitinger *et al.*, 2011). This suggests that phosphorylation of Hof1 by Dbf2 weakens the association between Hof1 and septins. To confirm this hypothesis, we performed in vivo pull-down assays using the established Hof1-4E mutant, in which four Dbf2 phosphorylation sites were mutated to glutamic acid to mimic phosphorylation (Figure 2A). For this analysis, we expressed *HOF1-3* hemagglutinin *(HA)* and *hof1-4E-3HA* in cells harboring the septin *CDC10* fused to the tandem and affinity purification (TAP) tag (Puig *et al.*, 2001; Figure 2B). In comparison to Hof1-3HA, 2.5-fold less Cdc10-TAP could be coimmunoprecipitated with Hof1-4E–3HA (Figure 2B), indicating that Hof1 phosphorylation at Dbf2 sites decreases the binding of Hof1 to septins.

We next asked whether Dbf2 specifically phosphorylated the SID region of Hof1. Of importance, one of the Dbf2 phosphorylation sites (RXXS) was present in the SID region (amino acids 310–313; Figure 2A). A single substitution of serine 313 to glutamic acid decreased the interaction between Hof1 and Cdc10 in the yeast two-hybrid system (Hof1-S313E) to a similar degree as the Hof1-4E mutations (Figure 2C; Meitinger *et al.*, 2011). This indicated that serine 313 is critical for the Hof1–septin interaction. This possibility was further evaluated by in vitro pull downs by using a bacterially purified septin complex and Hof1 truncations comprising amino acids 200–355 (Hof1-SID; Figure 2D; Versele and Thorner, 2004). In support of our model, glutathione *S*-transferase (GST)–Hof1-SID bound to the purified septins (Figure 2D). The degree of binding between GST–Hof1-SID-S313E and septins was significantly lower than to GST–Hof1-SID (Figure 2D). In line with this result, we observed that the levels of Hof1-S313E–green fluorescent protein (GFP) bound to septins were significantly diminished in metaphase-arrested cells (Figure 2E-G). In addition, Hof1-S313E–GFP prematurely shifted from septins to the AMR in anaphase-arrested cells. In contrast, in ~30% of wild-type cells, Hof1-GFP persisted at septins during the anaphase arrest (Figure 2, H and I). We therefore concluded that phosphorylation of serine 313 by Dbf2 kinase decreases the association of Hof1 with the septin complex both in vitro and in vivo.

The association of Hof1 with the septin scaffold was largely impaired upon deletion of the F-BAR domain in the *hof1-S313E* mutant (*hof1-Δ2-279-S313E*; Figure 2, J and K). These data are in agreement with our previous observation that both the F-BAR and SID domains are required for Hof1 colocalization with septins in vivo (Figure 1, E–G). The levels of Hof1 associated with septins were also reduced by the inactivation of the SH3 domain (W637A)

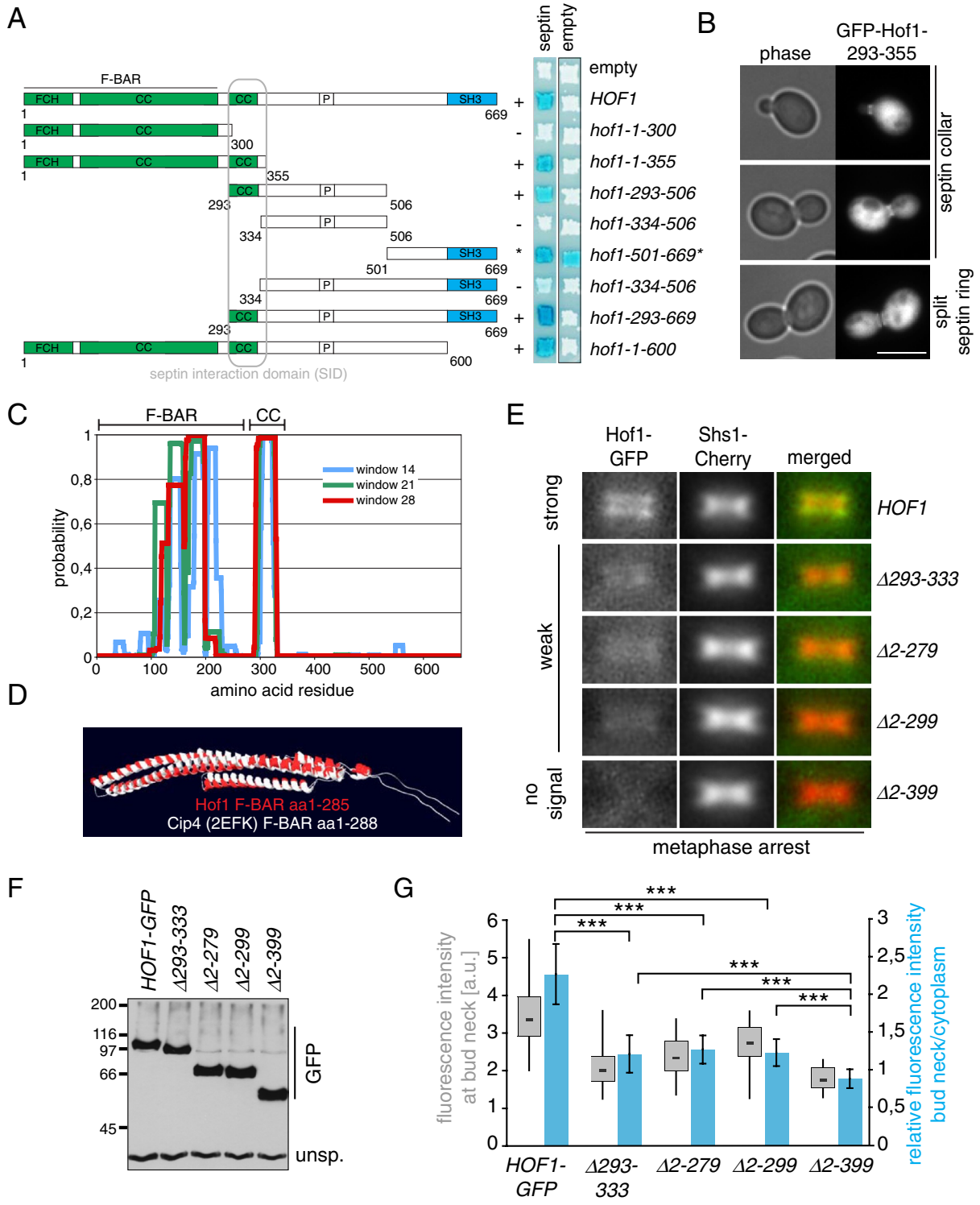

FIGURE 1: Mapping of the septin interaction domain of Hof1. (A) Yeast two-hybrid interactions between Hof1 fragments and septins (Cdc12). Blue color indicates interaction; asterisk, fragment is self-activating. (B) Localization of Hof1-293-355. Hof1-293-355 was overexpressed from the Gal1 promoter. Scale bar, 5 μm. (C) Graph shows probability of coiled-coil regions in Hof1. (D) In silico 3D model of the F-BAR domain of Hof1 in comparison to the resolved structure of the F-BAR domain of CIP4 as a reference. (E) Colocalization of Hof1-GFP, Hof1-Δ293-333–GFP, Hof1-Δ2-279–GFP, Hof1-Δ2-299–GFP, and Hof1-Δ2-399–GFP with the septin Shs1-Cherry in metaphase-arrested cells. (F) Immunoblot shows the amount of Hof1-GFP, Hof1-Δ293-333–GFP, Hof1-Δ2-279–GFP, Hof1-Δ2-299–GFP, and Hof1-Δ2-399–GFP in metaphase-arrested cells. An unspecific signal of the GFP antibody served as loading control. (G) Quantification of fluorescence intensity of Hof1-GFP ($n = 56$), Hof1-Δ293-333–GFP ($n = 39$), Hof1-Δ2-279–GFP ($n = 69$), Hof1-Δ2-299–GFP ($n = 50$), and Hof1-Δ2-399–GFP ($n = 34$) at the bud neck in metaphase-arrested cells. Blue bars, relative fluorescence intensity at the bud neck. Values >1 indicate an accumulation of Hof1 at the bud neck, whereas values <1 indicate no accumulation of Hof1 at the bud neck. Error bars, SD. *t* test, ***$p < 0.0001$.

alone (Hof1-W637A; Figure 2, J and K) and even more reduced when both W637A and S313E mutations were combined (*hof1-S313E-W637A*; Figure 2, J and K). This implied that the SH3 domain also plays a role in the localization of Hof1 at the septin complex, as previously suggested (Meitinger *et al.*, 2011). We therefore conclude that the F-BAR and SH3 domains, as well as the SID, contribute to the localization of Hof1 at the septin ring in vivo. However, we postulate that whereas the SID directly interacts with the septin scaffold in a phosphodependent manner, the F-BAR and SH3 domains contribute to the association of Hof1 with the septin scaffold by other means (Figure 2L).

Hof1 participates in the function of the septin complex

The fact that Hof1 associates with septins during most phases of the cell cycle (Lippincott and Li, 1998) led us to ask whether Hof1 regulates septin function and/or organization. To investigate this possibility, we assessed genetic interactions between *HOF1* and established upstream regulators of septin dynamics, including the protein kinases Cla4 and Gin4 and the protein phosphatase 2A (PP2A)–Rts1 complex (Dobbelaere *et al.*, 2003; Mortensen *et al.*, 2002; Versele and Thorner, 2004). Phosphorylation of septins by Cla4 and Gin4 stabilizes the septin complex at the bud neck, whereas dephosphorylation of Shs1 by Rts1 destabilizes septins during cytokinesis. Gin4 promotes septin stabilization through phosphorylation of Shs1 (Mortensen *et al.*, 2002). We found that the deletion of *HOF1* was lethal in the absence of *GIN4* (Figure 3A), which confirmed previous observations (Nishihama *et al.*, 2009). Neither deletion of the phosphatase gene *RTS1,* nor the *GIN4* orthologue kinases *HSL1* and *KCC4* (Dobbelaere *et al.*, 2003; Mortensen *et al.*, 2002) influenced the growth of *hof1*Δ cells (Figure 3B), suggesting that the genetic interaction between *GIN4* and *HOF1* was indicative of a specific interaction. Similarly, the absence of *CLA4* did not interfere with the growth of *hof1*Δ cells (Figure 3B). However, *hof1*Δ cells were synthetic lethal with the deletion of the Gin4 substrate encoded by *SHS1* (Figure 3C). Taken together, these findings indicate that Hof1 may stabilize septins by acting in a pathway that functions in parallel to the established control of Shs1 by Gin4.

To address the possibility that Dbf2 regulates the interaction between Hof1 and septins, we asked whether Hof1 mutants that harbor changes in the Dbf2-dependent phosphorylation sites affected the growth of *shs1*Δ or *gin4*Δ cells. Both *hof1-4E* and *hof1-S313E,* but not *hof1-4A,* were synthetically sick with *shs1*Δ and *gin4*Δ (Figure 3, A and C–E). Hof1 localization in *shs1*Δ and *gin4*Δ cells revealed that, in contrast to Hof1-GFP and Hof1-4A–GFP, association of Hof1-4E–GFP and Hof1-S313E–GFP signals were drastically reduced at the bud neck (Figure 3, F–I, and unpublished data). Instead the Hof1-4E–GFP and Hof1-S313E–GFP molecules mislocalized at the growing bud tip or mother cell cortex (Figure 3, F–I, arrows). Of importance, mislocalization of Shs1-GFP was significantly greater in *hof1-4E gin4*Δ than in *HOF1 gin4*Δ cells (Figure 3, J and K). In addition, *hof1-4E* or *hof1-S313E* cells lacking either *SHS1* or *GIN4* showed a strong morphology defect, as cells were elongated or enlarged (Figure 3, F and H). This indicated that phosphorylation of S313 inside the SID domain impairs Hof1's function in the absence of *GIN4* or *SHS1*. Taken together, our data suggest that there are two parallel pathways that control septin organization—one dependent on Gin4/Shs1 and the other on Dbf2/Hof1 (Figure 3L).

Phosphorylation of Hof1 at S313 induces rearrangement of septins

Given that Dbf2 phosphorylates Hof1 in late anaphase, we postulated that Hof1 phosphorylation might control the rearrangement of septins that accompanies cytokinesis (Figure 3L). To test this possibility, we arrested cells in late anaphase and monitored the localization of both Hof1 and septins (Figure 4). The late-anaphase arrest was achieved either through overexpression of the nondegradable B-type cyclin Clb2 (*clb2ΔDB*; Surana *et al.*, 1993) or through inactivation of the MEN by shifting *dbf2-2 dbf20*Δ cells to the restrictive temperature. As previously shown (Meitinger *et al.*, 2011), Hof1-GFP or Hof1-4A–GFP colocalized with septins, whereas Hof1-4E–GFP was prematurely dislodged from septins and relocated to the AMR in the anaphase-arrested cells. Of interest, after an anaphase arrest of 6 h (*clb2ΔDB*), the septin collar-like structure collapsed to one side of the bud neck, forming a half-moon structure in *hof1-4E* but not in *HOF1* or *hof1-4A* cells (Figure 4A). This phenotype was specific for S313E, as it was not observed in *hof1-S421E* or *hof1-S533E-S563E* cells (Figure 4, A and B). Similar results were obtained for anaphase-arrested *dbf2-2 dbf20*Δ cells (Figures 4, C–E). Of importance, Hof1-4E–GFP and Hof1-S313E–GFP protein levels remained constant throughout the prolonged anaphase arrest (Figure 4D), indicating that cells did not enter the G1 phase, where Hof1 is degraded (Blondel *et al.*, 2005). We also observed that Hof1-S313E–GFP and Hof1-4E–GFP, but not Hof1-GFP, mislocalized to the cell cortex in a fraction of *dbf2-2 dbf20*Δ–arrested cells (Figure 4, C and F). In addition, the increase in the proportion of *hof1-4E dbf2-2 dbf20*Δ cells, in which the septin ring collapsed or was mislocalized, directly correlated with the decrease in the survival rate of these cells when compared with the control *HOF1 dbf2-2 dbf20*Δ (Figure 4G). Of note, asymmetric septin collapse at the bud neck was reported for cells lacking the septin *CDC10* (Versele and Thorner, 2005), suggesting that Hof1 may act like Cdc10 to stabilize the septin collar. However, the deletion of *HOF1* had no effect on septin rearrangement in *clb2ΔDB*-arrested cells (unpublished data). We postulated that *hof-4E* or *hof1-S313E* mutants might have a remaining F-BAR– or SH3-dependent activity, which would induce septin rearrangement. We tested this hypothesis by inactivating the F-BAR (Δ2-279) or SH3 (W637A) domain in combination with the S313E mutation. In addition, we analyzed Hof1 truncated forms that lacked both F-BAR and SID (Δ2-399) domains (Figure 4H). We found that a high percentage of cells with asymmetric septin rings accumulated in *hof1-S313E* and *hof1-Δ293-332* cells (50–60%; Figure 4H). In contrast, asymmetric septin localization was barely observed in mutants that lacked a functional F-BAR or SH3 domain (W637A, Δ2-279, Δ2-229, Δ2-399; Figure 4H). Of importance, the inactivation of F-BAR or SH3 function rescued the asymmetric septin localization defects observed in *hof1-S313E* and *hof1-Δ293-332* cells (S313E-W637A and Δ2-279-S313E; Figure 4H), although these truncations completely failed to localize at the bud neck (Figure 4I). We concluded that the persistence of Hof1-S313E at the bud neck causes septin disorganization in an F-BAR– and SH3-domain–dependent manner.

Hof1 phosphorylation at positions S533 and S563 by Dbf2 is essential for AMR contraction and septum formation

We previously reported that deletion of *CYK3* in *hof1-4A* cells is lethal (Meitinger *et al.*, 2011). This lethality was based on alanine substitutions at positions S533 and S563 but not at positions S313 or S421 or any other putative Dbf2 phosphorylation site (Supplemental Figure S1A; Meitinger *et al.*, 2011). Of importance, both S533 and S563 were phosphorylated by Dbf2-Mob1 in vitro (Supplemental Figure S1, B and C). We therefore concluded that the phosphorylation of S533 and S563 by Dbf2-Mob1 promotes a function of Hof1 that is independent of S313 and hence is not related to the SID.

To investigate which function of Hof1 is impaired in the absence of Cyk3, we established a system in which Cyk3 depletion can be

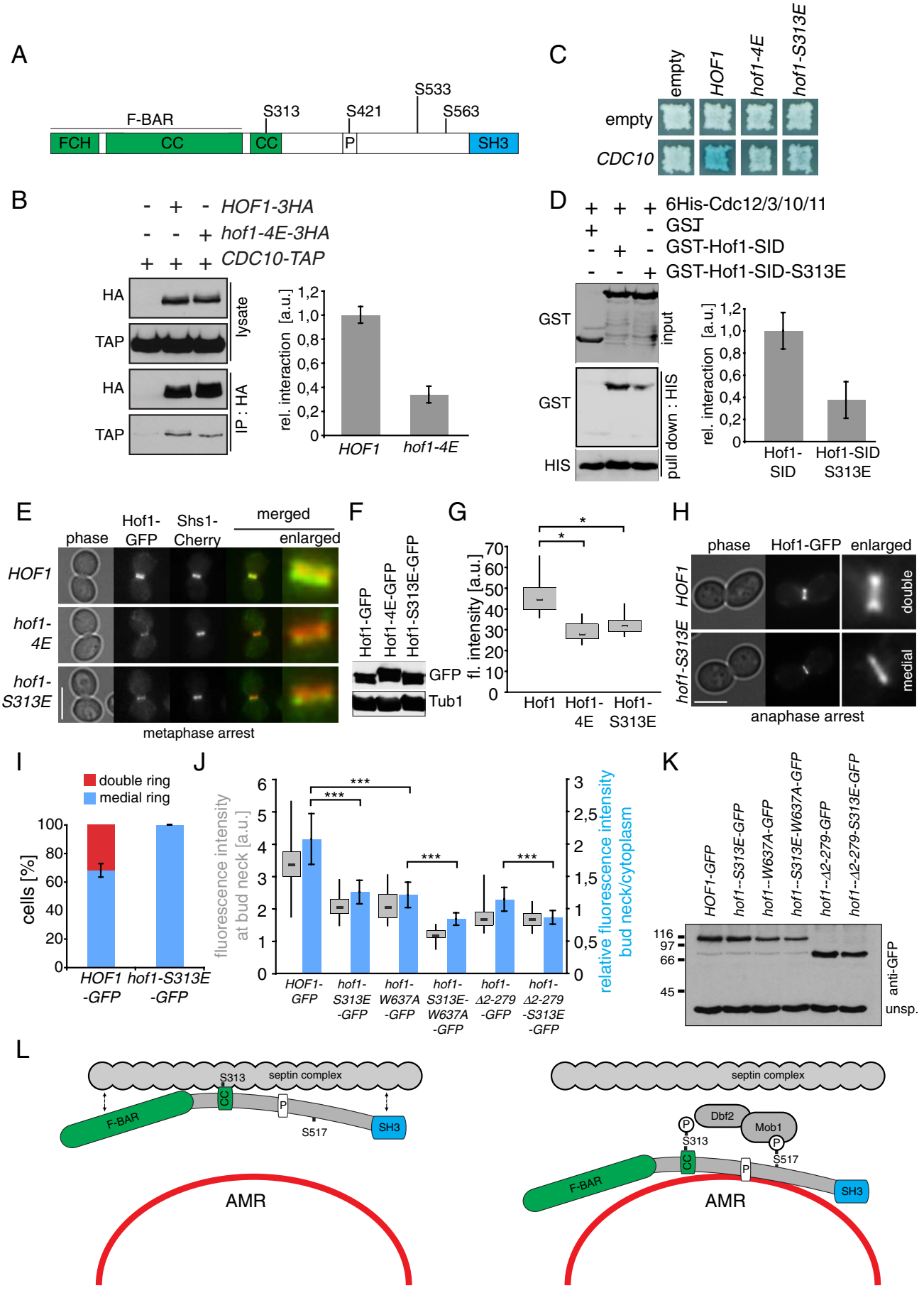
A
F-BAR
S313
S421
S533
S563
FCH
CC
CC
P
SH3
B
- + - HOF1-3HA
- - + hof1-4E-3HA
+ + + CDC10-TAP
HA
TAP
HA
TAP
lysate
IP : HA
rel. interaction [a.u.]
1,2
1,0
0,8
0,6
0,4
0,2
0
HOF1
hof1-4E
C
empty
HOF1
hof1-4E
hof1-S313E
empty
CDC10
D
+ + + 6His-Cdc12/3/10/11
+ - GST
- + - GST-Hof1-SID
- - + GST-Hof1-SID-S313E
GST
GST
HIS
input
pull down : HIS
rel. interaction [a.u.]
1,2
1,0
0,8
0,6
0,4
0,2
0
Hof1-SID
Hof1-SID S313E
E
phase
Hof1-GFP
Shs1-Cherry
merged
enlarged
HOF1
hof1-4E
hof1-S313E
metaphase arrest
F
Hof1-GFP
Hof1-4E-GFP
Hof1-S313E-GFP
GFP
Tub1
G
fl. intensity [a.u.]
70
60
50
40
30
20
10
0
*
*
Hof1
Hof1-4E
Hof1-S313E
H
phase
Hof1-GFP
enlarged
HOF1
hof1-S313E
double
medial
anaphase arrest
I
double ring
medial ring
cells [%]
100
80
60
40
20
0
HOF1 -GFP
hof1-S313E -GFP
J
fluorescence intensity at bud neck [a.u.]
6
5
4
3
2
1
0
***
***
***
***
relative fluorescence intensity bud neck/cytoplasm
3
2,5
2
1,5
1
0,5
0
HOF1-GFP
hof1-S313E-GFP
hof1-W637A-GFP
hof1-S313E-W637A-GFP
hof1-Δ2-279-GFP
hof1-Δ2-279-S313E-GFP
K
HOF1-GFP
hof1--S313E-GFP
hof1--W637A-GFP
hof1--S313E-W637A-GFP
hof1--Δ2-279-GFP
hof1--Δ2-279-S313E-GFP
116
97
66
45
anti-GFP
unsp.
L
S313
septin complex
F-BAR
CC
P
S517
SH3
AMR
septin complex
Dbf2
Mob1
P
S313
P
S517
F-BAR
CC
P
SH3
AMR

induced, resulting in temperature-dependent lethality (Figure 5, A and B). Given that Hof1 has an established role in promoting AMR contraction and/or septum formation (Lippincott and Li, 1998; Meitinger *et al.*, 2011), we postulated that phosphorylation of S533 and S563 by Dbf2 might impinge upon this function.

To obtain better insight into the functional consequences of Hof1 phosphorylation by Dbf2, we analyzed the phenotype of nonphosphorylatable mutations of *HOF1*, *hof1-4A*, in cells carrying *CYK3* under control of the inducible galactose promoter (pGal1-*3HA-CYK3*). Repression of pGal1-*3HA-CYK3* upon glucose addition led to Cyk3 depletion (Figure 5C). Ultrastructure analysis of the bud neck region by transmission electron microscopy (TEM) showed that a substantial proportion (19%) of the observed *hof1-4A* pGal1-*3HA-CYK3* cells initiated a new cell cycle (rebudding) in spite of the fact that the primary and secondary septa were not closed (open septum, Figure 5D). Hof1-4A–GFP localization in cells lacking Cyk3 showed that Hof1-4A–GFP formed a ring that did not contract (Figure 5F, 1–3, white arrows) and persisted at the old bud neck during the following cell cycle (Figure 5F, 4 and 5, white arrows). In contrast, Hof1-GFP disappeared from the bud neck after septin splitting and AMR contraction (Figure 5E, asterisk). This persistent localization of Hof1-4A–GFP in Cyk3-depleted cells indicated that Hof1-4A might form a tight association with the bud neck. Of interest, the Hof1-interacting protein Inn1 and primary septum synthase subunit Chs2, a downstream effector of the Hof1–Inn1 complex (Nishihama *et al.*, 2009), also remained associated with the AMR. This suggested that AMR contraction and primary septum formation are, in general, impaired in Cyk3-depleted *hof1-4A* cells (Supplemental Figure S2). These defects are unlikely to arise from septin ring reorganization, as septin splitting took place in both *HOF1* and *hof1-4A* pGal1-*CYK3* cells (Figure 5F, 2, 4, and 5). We conclude that phosphorylation of Hof1 by Dbf2 at the end of mitosis is required to trigger AMR contraction and primary septum (PS) formation.

Hof1 inhibits AMR contraction and PS formation via its SH3 domain

We hypothesized that phosphorylation of Hof1 by Dbf2 promotes AMR contraction. Consequently one would expect that AMR contraction should be impaired in the nonphosphorylatable *hof1-4A* mutant. To test this hypothesis, we analyzed the dynamics of AMR contraction by time-lapse microscopy in *hof1-4A* with Cyk3 either present or absent. Because the tagging of Myo1 made cells lacking Cyk3 sick, we followed the constriction of Hof1-GFP (wild type or phosphomutants), which is a well-established associated component of the contractile AMR (Lippincott and Li, 1998; Young *et al.*, 2010). In cells expressing *CYK3*, Hof1-4A–GFP and Hof1-4E–GFP behaved in a similar manner by finishing AMR contraction latest 10 min after Hof1 recruitment (Figure 6, A, B, and C, 1), which is consistent with the timing of Myo1-GFP contraction under the same conditions (Tully *et al.*, 2009). The timing of Hof1-GFP constriction was extended to ~20 min when Cyk3 had been depleted (Figure 6, A, B, and C, 2). This indicates that the presence of Cyk3 is required for proper AMR contraction. Whereas Hof1-4E–GFP and Hof1-S313A–GFP behaved like Hof1-GFP, Hof1-4A–GFP and Hof1-S533A-S563A–GFP constriction was drastically retarded upon *CYK3* depletion (Figure 6, A, B, and C, 3). A similar defect in AMR contraction was observed in *hof1-S517A-GFP* cells (Figure 6, A, C, and D), in which Hof1-S517A inefficiently binds to Mob1, thereby impeding S533 and S563 phosphorylation (Meitinger *et al.*, 2011). Of interest, the duration of AMR contraction correlated with cell death, as the percentage of death events significantly increased with the increasing duration of AMR contraction (Figure 6D). In line with these data, we observed that cells died during prolonged AMR constriction (Figure 6E). Of importance, cell death was never observed during other cell cycle phases. Taken together, our data indicate that both Cyk3 and Dbf2-phosphorylated Hof1 are required for the efficient contraction of the AMR, which is important to maintain cell integrity during cytokinesis.

We next asked how Hof1 regulates AMR contraction in a phosphorylation-dependent manner. The C-terminal SH3 domain of Hof1 binds actin nucleation factors, thereby inhibiting cytokinesis (Ren *et al.*, 2005). One possibility is that phosphorylation of Hof1 by Dbf2 influences the function of the SH3 domain. To test this hypothesis, we inactivated the SH3 domain by mutating the conserved tryptophan 637 to alanine (Hof1-W637A; Meitinger *et al.*, 2011). This mutation had no effect on cell growth in either the presence or absence of *CYK3* (Figure 6, F, lane 5, and G, lanes 2 and 4).

FIGURE 2: Phosphorylation regulates the direct interaction of Hof1 with septins. (A) Hof1 domains and Dbf2-specific phosphorylation sites are depicted. F-BAR, Fes/CIP4 homology-Bin/Amphiphysin/Rvsp; CC, coiled-coil region; P, PEST motif. (B) Immunoprecipitation between Hof1 wild type or Hof1-4E and Cdc10. The graph shows the relative interaction of Hof1 and Hof1-4E with Cdc10 from two independent experiments. Error bars, SD. (C) Yeast two-hybrid interaction of Hof1, Hof1-4E, and Hof1-S313E with the septin Cdc10. Blue color indicates interaction. (D) In vitro pull down between Hof1-CC (codons 200–355) or Hof1-CC-S313E and the septin complex (6His-Cdc12-Cdc3-Cdc10-Cdc11). The graph shows the relative interaction of Hof1 and Hof1-4E with the septin complex from four independent experiments. Error bars represent SD. (E) Colocalization of Hof1-GFP, Hof1-4E–GFP, and Hof1-S313E–GFP with the septin Shs1 in metaphase-arrested cells. (F) Immunoblot shows the amount of Hof1-GFP, Hof1-4E–GFP, and Hof1-S313E–GFP in metaphase-arrested cells. (G) Quantification of fluorescence intensity of Hof1-GFP ($n = 15$), Hof1-4E–GFP ($n = 15$), and Hof1-S313E–GFP at the bud neck in metaphase-arrested cells. *t* test, $*p < 0.01$. (H) Localization of Hof1-GFP and Hof1-S313E–GFP in anaphase-arrested cells. (I) Quantification of Hof1 and Hof1-S313E localization in anaphase-arrested cells. Three independent experiments were quantified ($n > 100$ per strain). Error bars, SD. (J) Quantification of fluorescence intensity of Hof1-GFP ($n = 37$), Hof1-S313E–GFP ($n = 28$), Hof1-W637A–GFP ($n = 30$), Hof1-S313E–W637A ($n = 31$), Hof1-Δ2-279–GFP ($n = 33$), and Hof1-Δ2-279-S313E–GFP ($n = 30$) at the bud neck in metaphase-arrested cells. Blue bars, relative fluorescence intensity at the bud neck. Values >1 indicate an accumulation of Hof1 at the bud neck, whereas values <1 indicate no accumulation of Hof1 at the bud neck. *t* test, $***p < 0.0001$. (K) Immunoblot shows the amount of Hof1-GFP, Hof1-S313E–GFP, Hof1-W637A–GFP, Hof1-S313E-W637A, Hof1-Δ2-279–GFP, and Hof1-Δ2-279-S313E–GFP in metaphase-arrested cells. An unspecific signal of the GFP antibody served as loading control. (L) Model for Hof1 regulation. During anaphase Hof1 associates with the septin collar. On prephosphorylation of S517 by Cdc5, the Dbf2-Mob1 complex binds to Hof1 and phosphorylates S313, thereby resolving Hof1 from the septin collar. F-BAR and SH3 domain contribute to the association of Hof1 with the septin collar by an unknown mechanism. Scale bars, 5 μm.

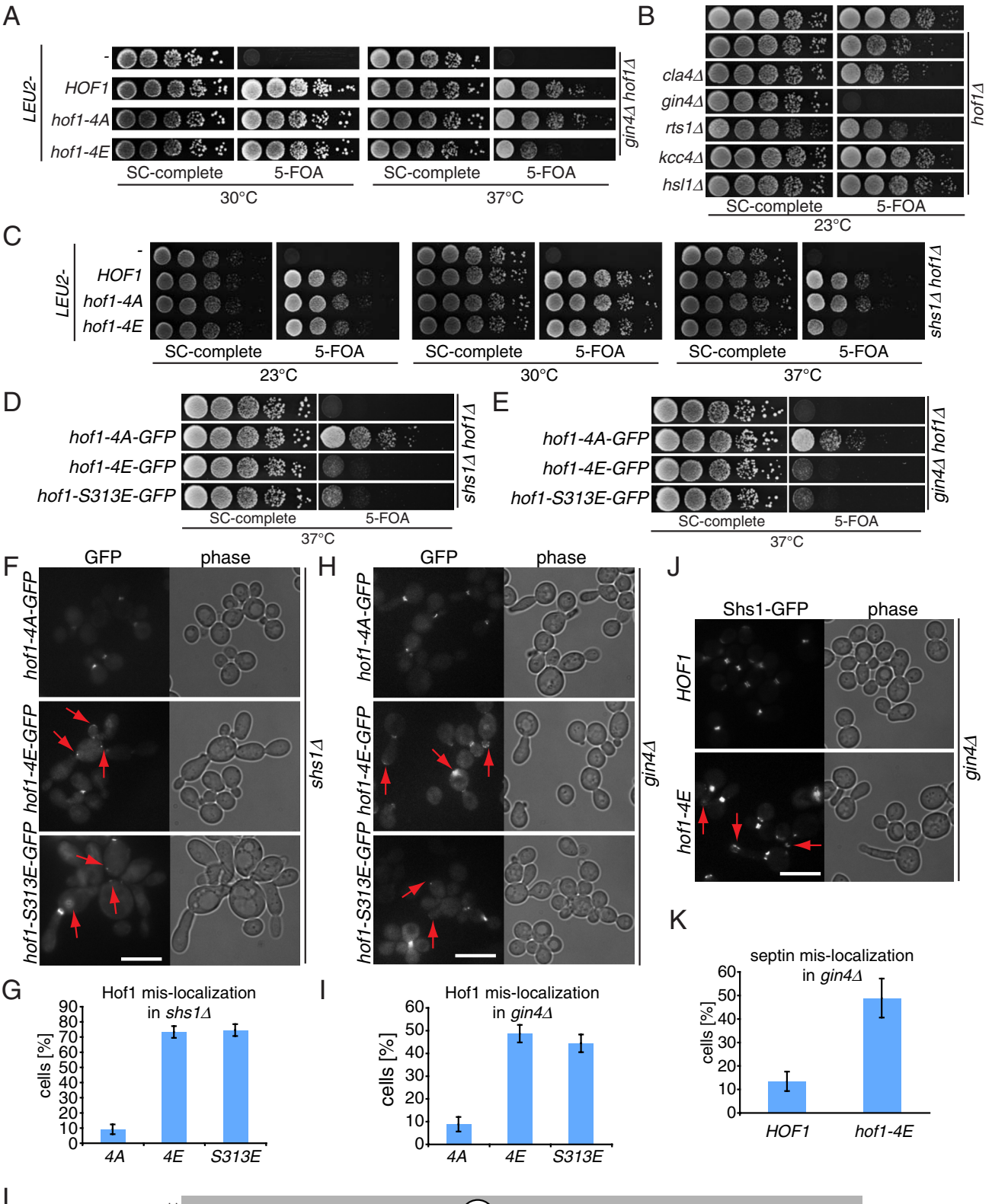
A
LEU2-
-
HOF1
hof1-4A
hof1-4E
gin4Δ hof1Δ
SC-complete
5-FOA
SC-complete
5-FOA
30°C
37°C
B
cla4Δ
gin4Δ
rts1Δ
kcc4Δ
hsl1Δ
hof1Δ
SC-complete
5-FOA
23°C
C
LEU2-
-
HOF1
hof1-4A
hof1-4E
shs1Δ hof1Δ
SC-complete
5-FOA
SC-complete
5-FOA
SC-complete
5-FOA
23°C
30°C
37°C
D
hof1-4A-GFP
hof1-4E-GFP
hof1-S313E-GFP
shs1Δ hof1Δ
SC-complete
5-FOA
37°C
E
hof1-4A-GFP
hof1-4E-GFP
hof1-S313E-GFP
gin4Δ hof1Δ
SC-complete
5-FOA
37°C
F
GFP
phase
hof1-4A-GFP
hof1-4E-GFP
hof1-S313E-GFP
shs1Δ
H
GFP
phase
hof1-4A-GFP
hof1-4E-GFP
hof1-S313E-GFP
gin4Δ
J
Shs1-GFP
phase
HOF1
hof1-4E
gin4Δ
K
septin mis-localization
in gin4Δ
cells [%]
60
50
40
30
20
10
0
HOF1
hof1-4E
G
Hof1 mis-localization
in shs1Δ
cells [%]
90
80
70
60
50
40
30
20
10
0
4A
4E
S313E
I
Hof1 mis-localization
in gin4Δ
cells [%]
60
50
40
30
20
10
0
4A
4E
S313E
L
before mitotic exit
stabilized septins:
collar structure
after mitotic exit
unstable septins:
septin splitting
and rearrangment
P
Shs1
Gin4
Rts1
Shs1
?
Hof1
P
Hof1
Dbf2

Furthermore, the Hof1-W637A–GFP ring contracted at similar rates to that of wild-type Hof1-GFP (Figure 6A). Of interest, cells in which both the SH3 domain and the Dbf2 phosphorylation sites of Hof1 were inactivated (*hof1-4A-W637A*, *hof1-S533A-S563A*, and *hof1-S517A* cells) were able to grow in the absence of *CYK3* (Figure 6, F, lane 6, and G, lanes 6 and 8). These cells were proficient in AMR contraction, like wild-type cells (Figure 6A). This indicates that the SH3 domain of Hof1 exerts an inhibitory influence over AMR contraction. Collectively our results show that phosphorylation of Hof1 by Dbf2 contributes to AMR contraction and primary septum formation, most likely through inhibition of the SH3 domain (Figure 6H).

Hof1 phosphorylation defects can be bypassed by promoting PS formation or inhibiting PS degradation

After cytokinesis (i.e., after AMR contraction and septa closure), a set of hydrolases partially digests the septum to separate the daughter from the mother cell (Colman-Lerner *et al*., 2001). In wild-type cells, hydrolase expression is coupled to cell cycle progression in such a way that their expression starts at the same time as AMR contraction and the formation of the primary septum are triggered (Brace *et al*., 2011). The observation that AMR contraction and septum formation were delayed in *hof1-4A* Cyk3-depleted cells (Figures 5 and 6), together with the fact that a large percentage of cells died during ring constriction (Figure 6, D and E), led us to ask whether cell death could arise from the action of hydrolases on the incompletely closed septum. Indeed, we observed by TEM analysis that cell separation was initiated in *hof1-4A* Cyk3-depleted with an open septum (Figure 7A, arrows). In agreement with our hypothesis, the deletion of a set of hydrolases (*CTS1*, *EGT2*, *DSE2*, and *SWC11*) restored viability to *hof1-4A cyk3*Δ cells (Figure 7B).

We postulated that promotion of primary septum formation in *hof1-4A cyk3*Δ cells would speed up septum closure before the hydrolases could act on the compromised septum to also revert the lethality. To assess this possibility, we ectopically overproduced the primary septum–synthesizing enzyme Chs2 or its putative activator Inn1 in *hof1-4A cyk3*Δ cells. Both *CHS2* and *INN1* overexpression partially rescued the growth defect of *hof1-4A cyk3*Δ cells (Figure 7C), indicating that timely coordination of septum closure and resolution is critical for cell viability. Taken together, our data indicate that Dbf2 phosphorylates Hof1, which, together with Cyk3, efficiently promotes AMR contraction and primary septum formation before the onset of cell separation.

DISCUSSION

During cytokinesis, a variety of signals need to be integrated to coordinate cell division with cell cycle progression and coordinate the action of the different molecular machineries that are necessary to complete cell separation. In spite of the considerable progress made toward the characterization of cytokinetic components in budding yeast, we know very little about the means by which the function of the cytokinetic machinery is coupled to the cell cycle signals to ensure that cell division occurs at the correct time. Here we build upon previous work that established the F-BAR protein Hof1 as a bona fide substrate of the cell cycle regulatory NDR kinase Dbf2 (Meitinger *et al*., 2011). We show that Dbf2 kinase regulates two functionally distinct domains of Hof1 independently. Our data suggest a novel role for Hof1 in septin organization and highlight the importance of Dbf2 in the coordination of septin and AMR functions via Hof1.

Hof1 binds to and regulates septins

Dbf2 localizes at the cell division site shortly before the onset of AMR contraction (Frenz *et al*., 2000). We previously showed that Dbf2 phosphorylates Hof1 on several sites between the N-terminal F-BAR and C-terminal SH3 domains. Dbf2 phosphorylation on Hof1 resolves Hof1 from the septin scaffold, allowing association with the AMR, which, in turn, promotes AMR constriction (Frenz *et al*., 2000; Luca *et al*., 2001; Meitinger *et al*., 2011). Our data now show that Dbf2 regulates two independent domains of Hof1. Using the yeast two-hybrid system and in vivo and in vitro pull downs, we first established that Hof1 directly interacts with the septin complex via a coiled-coil region, which we named as SID, for septin interaction domain. Of importance, 3D modeling revealed that, although the SID domain is close to the conserved F-BAR domain, it is not part of it. Our data demonstrate that the SID-mediated interaction between Hof1 and septins is controlled by phosphorylation of a single Dbf2 phosphorylation site (serine 313) within the SID domain. The constitutive phosphomimetic mutation S313E impaired Hof1's association with septins through this domain both in vitro and in vivo. Of interest, Imp2, which is one of the two homologues of Hof1 in fission yeast (Demeter and Sazer, 1998), has a predicted coiled-coil domain next to its F-BAR domain, suggesting that the underlying mechanisms of Hof1 regulation described here may be conserved in other organisms.

The finding that Hof1-S313E prematurely dissociates from the septin collar during anaphase allowed us to specifically investigate whether Hof1 executed a function in septin organization. Our data point toward a role for Hof1 in the stabilization of the septin scaffold complex. Genetic analysis showed that *hof1-S313E* cells were unable to survive in the absence of the septin-stabilizing kinase Gin4 or its substrate Shs1. Moreover, Shs1 localization was severely perturbed in *HOF1*-knockout or *hof1-S313E* cells lacking Gin4, indicating that Hof1 contributes to septin stabilization in a pathway that acts in parallel to Gin4. We propose that Hof1 in the Dbf2 hypophosphorylated state is maintained at the septin complex and contributes to septin integrity until the onset of AMR contraction. The fact that Dbf2 translocates to the bud neck shortly before the AMR starts to constrict indicates that Hof1 might stabilize the septin ring until Dbf2 arrives at the bud neck, a point at which the phosphorylation of Hof1 by Dbf2 inhibits the binding of Hof1 to septins via its SID domain.

FIGURE 3: Hof1 regulates the septin complex. (A) Genetic interaction of *hof1*Δ, *hof1-4A*, and *hof1-4E* with *gin4*Δ. (B) Genetic interaction of *hof1*Δ with regulators of septin dynamic *cla4*Δ, *gin4*Δ, *rts1*Δ, *kcc4*Δ, and *hsl1*Δ. (C) Genetic interaction of *hof1*Δ, *hof1-4A*, and *hof1-4E* with *shs1*Δ. (D, E) Genetic interaction of *hof1*Δ, *hof1-4A*, *hof1-4E*, and *hof1-S313E* with *gin4*Δ and *shs1*Δ. (F) Localization of Hof1-4A–GFP, Hof1-4E–GFP, and Hof1-S313E–GFP in *shs1*Δ strains. Cells were grown at 30°C. Arrows indicate mislocalization of Hof1. (G) Quantification of F. Two independent experiments were quantified ($n > 100$ per strain and experiment). Error bars, SD. (H) Localization of Hof1-4A–GFP, Hof1-4E–GFP, and Hof1-S313E–GFP in *gin4*Δ strains. Cells were grown at 30°C. Arrows indicate mislocalization of Hof1. (I) Quantification of H. Two independent experiments were quantified ($n > 100$ per strain and experiment). Error bars, SD. (J) Localization of Shs1-GFP in *gin4*Δ and *hof1-4E gin4*Δ mutants. Arrows indicate mislocalization of Shs1. (K) Quantification of J. Three independent experiments were quantified ($n > 100$ per strain and experiment). Error bars, SD. (J) Model for regulation of septin stability. Scale bars, 10 μm.

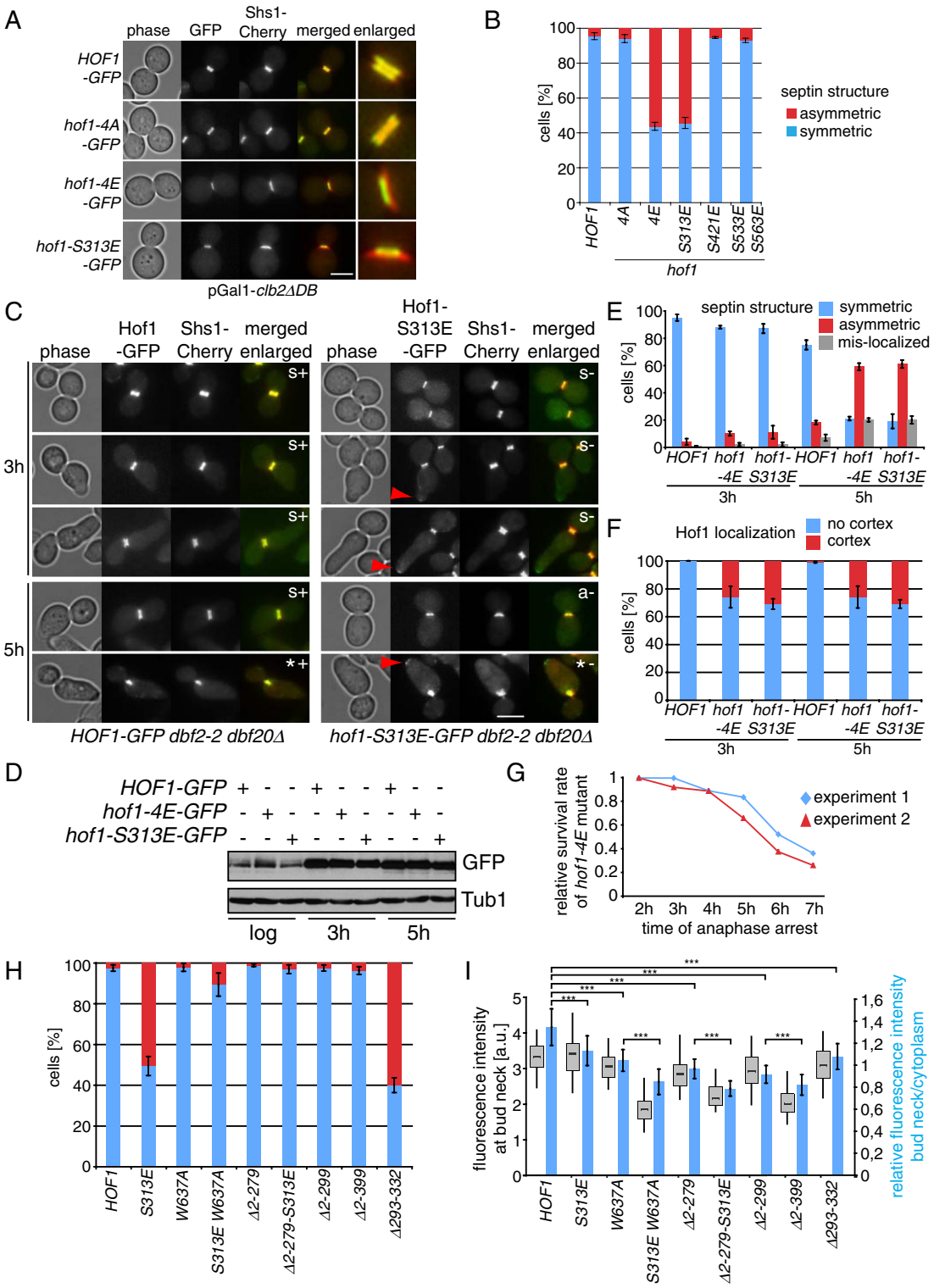

FIGURE 4: Hof1 phosphorylation induces septin rearrangement. (A) Localization of Shs1-Cherry in *HOF1-GFP*, *hof1-4A-GFP*, *hof1-4E-GFP*, and *hof1-S313E* mutants after prolonged anaphase arrest (pGal1-*clb2ΔDB*, 6 h). (B) Quantification of asymmetric Shs1-Cherry localization in *HOF1-GFP*, *hof1-4A-GFP*, *hof1-4E-GFP*, *hof1-S313E*, *hof1-S421E*, and *hof1-S533E-S563E* mutants after prolonged anaphase arrest (pGal1-*clb2ΔDB*, 6 h). Three independent experiments were quantified ($n > 100$ per strain and experiment). Error bars, SD. (C) Localization of Hof1-GFP and Hof1-S313E–GFP in comparison to Shs1-Cherry in anaphase-arrested cells (*dbf2-2 dbf20Δ*). Cycling cells were shifted from 23 to 37°C to arrest them in anaphase for 5 h. Samples were taken after 3 and 5 h to analyze septin localization, Hof1 localization, and protein amounts. Red arrowhead indicates mislocalization of Hof1-S313E–GFP to the cell cortex; a, asymmetric septin structure, s, symmetric septin structure; *, mislocalization of septin structure; +, complete colocalization of Hof1-GFP and Shs1-Cherry; –, no complete colocalization of Hof1-GFP and Shs1-Cherry. (D) Immunoblot shows the protein levels of Hof1-GFP, Hof1-4E–GFP, and Hof1-S313E during the course of the

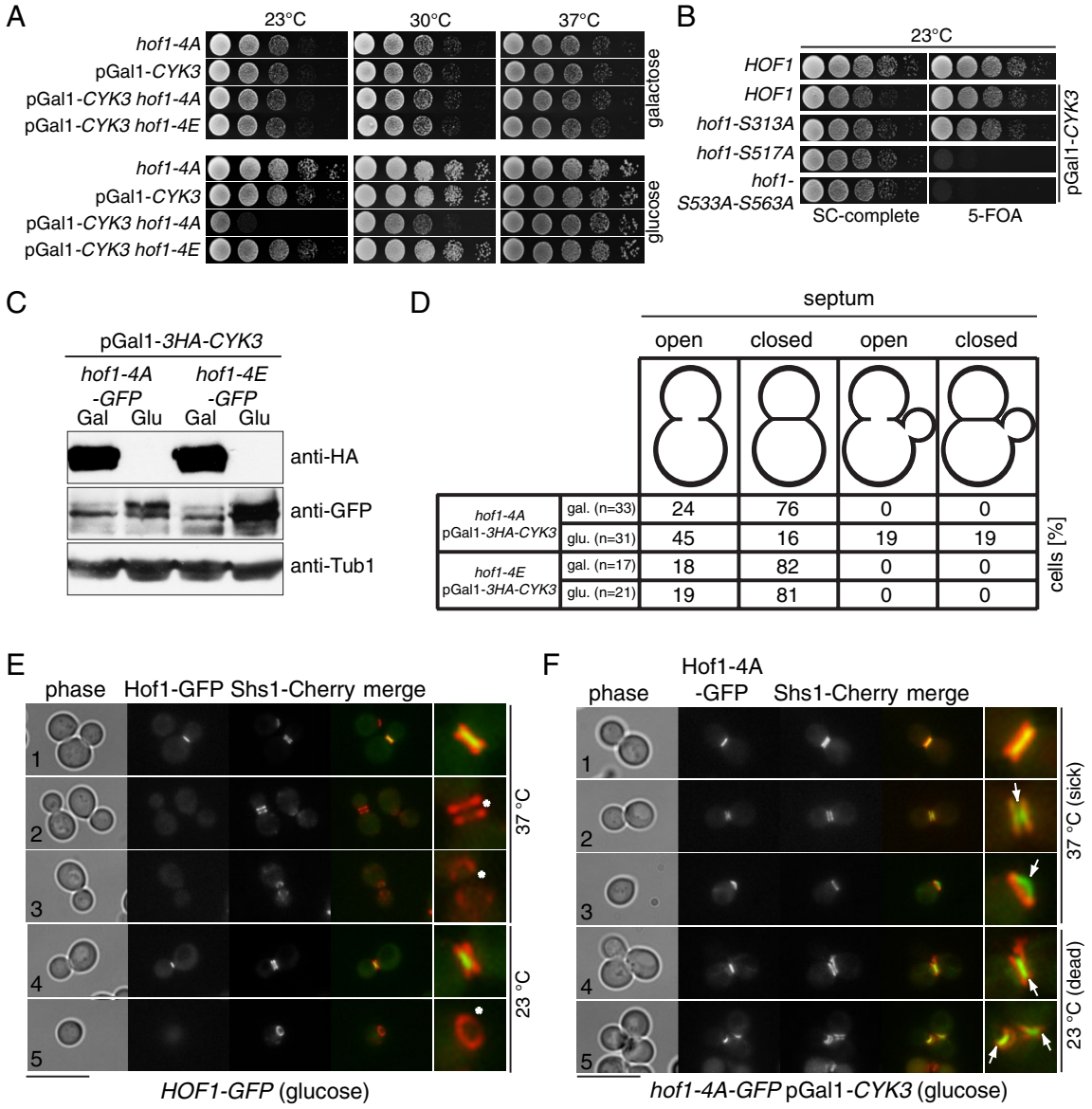

FIGURE 5: Hof1 phosphorylation is essential for AMR contraction and septum formation. (A) Genetic interactions are shown between the indicated Hof1 mutants with expression (galactose) or repression (glucose) of pGAL-*CYK3* at different temperatures. (B) Genetic interactions of the indicated genotypes. Cells contain an *URA3*-based plasmid carrying wild-type *CYK3* and were grown in glucose (2%)-containing medium at 23°C. Serial dilutions were spotted onto glucose (2%)-containing plates without or with 5-FOA. 5-FOA selects against the *URA3*-based plasmid carrying wild-type *CYK3*. Plates were incubated at 23°C. (C, D) Repression of pGAL-*CYK3* causes cytokinesis defects in *hof1-4A* but not in *hof1-4E* cells. Quantification of cells with open and closed septa. Septa were analyzed with a TEM. (E, F) Localization of Hof1-GFP and Hof1-4A–GFP after repression of pGAL-*CYK3*. The septin Shs1 fused to Cherry served as cell cycle marker (collar, before mitotic exit; split rings, after mitotic exit). Asterisk, Hof1 disappears from the bud neck after septin splitting; arrows, Hof1-4A is stabilized between the split septin rings. Scale bars, 10 μm.

experiment (anaphase arrest). (E) Quantification of septin structures as indicated during prolonged anaphase arrest. Three independent experiments were quantified ($n > 100$ per strain and experiment). Error bars, SD. (F) Quantification of Hof1 localization as indicated during prolonged anaphase arrest. Three independent experiments were quantified ($n > 100$ per strain and experiment). Error bars, SD. (G) Graph shows the survival rate of *hof1-4E-GFP* mutant cells relative to *HOF1-GFP* wild-type cells (see *Materials and Methods*). (H) Quantification of asymmetric Shs1-Cherry localization in the indicated Hof1 mutants after prolonged anaphase arrest (pGal1-*clb2ΔDB*, 6 h). Three independent experiments were quantified ($n > 100$ per strain and experiment). Error bars, SD. (I) Quantification of Hof1-GFP ($n = 38$), Hof1-S313E–GFP ($n = 35$), Hof1-W637A–GFP ($n = 38$), Hof1-S313E-W637A–GFP ($n = 36$), Hof1-Δ2-279–GFP ($n = 36$), Hof1-Δ2-279-S313E–GFP ($n = 38$), Hof1-Δ2-299–GFP ($n = 35$), Hof1-Δ2-399–GFP ($n = 37$), and Hof1-Δ293-333–GFP ($n = 38$) at the bud neck after prolonged anaphase arrest (pGal1-*clb2ΔDB*, 6h). Blue bars, relative fluorescence intensity at the bud neck. Values >1 indicate an accumulation of Hof1 at the bud neck, whereas values <1 indicate no accumulation of Hof1 at the bud neck. Error bars, SD. *t* test, $^{***}p < 0.0001$. Scale bars, 5 μm.

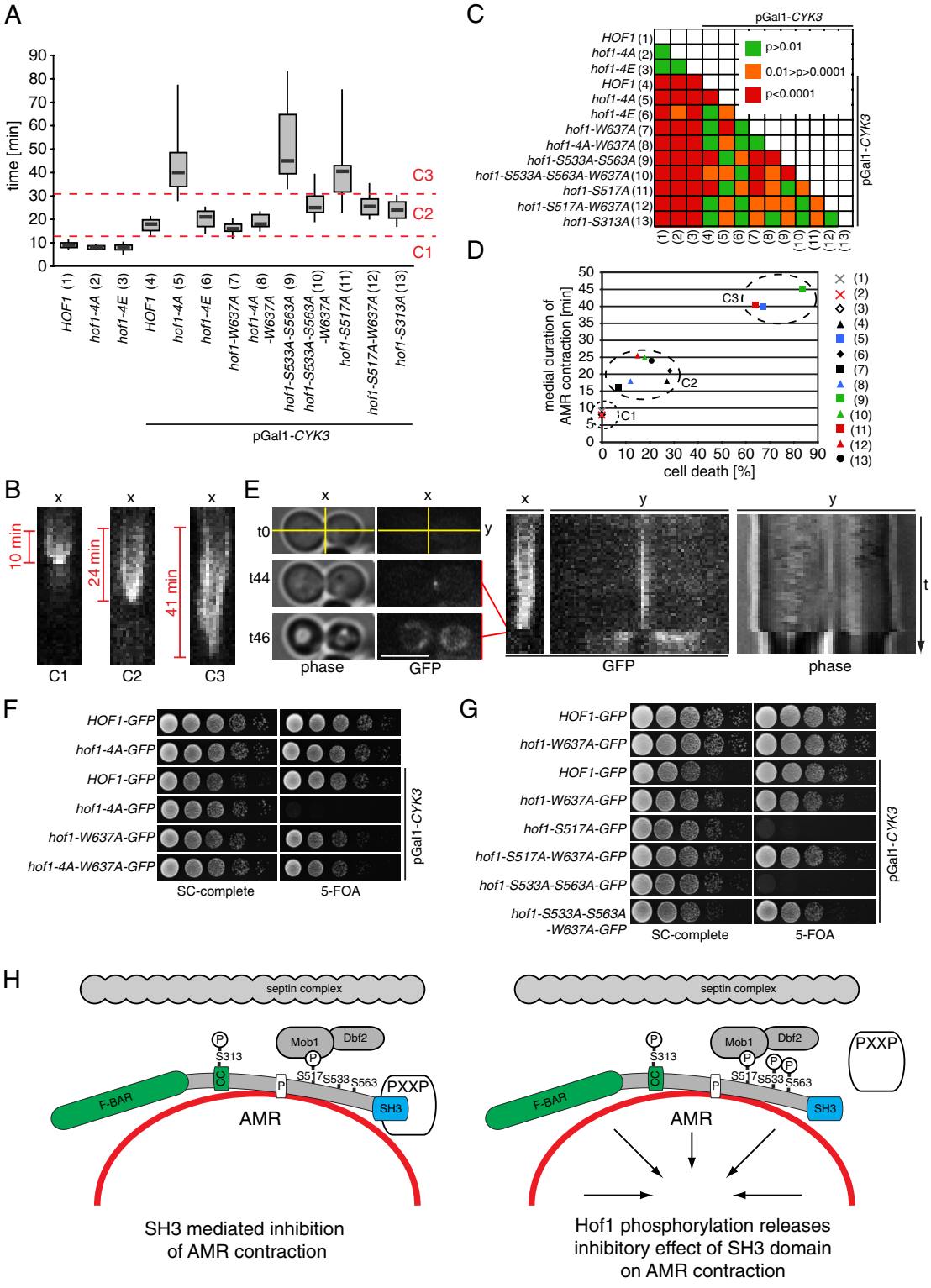

FIGURE 6: Hof1 inhibits AMR contraction and PS formation via its SH3 domain. (A) Quantification of the duration of Hof1 (wild type or indicated mutant) appearance at the AMR until completion of AMR contraction (see B for representative images). *HOF1-GFP* ($n = 8$), *hof1-4A-GFP* ($n = 6$), *hof1-4E-GFP* ($n = 16$), *HOF1* pGal1-*CYK3* ($n = 10$), *hof1-4A-GFP* pGal1-*CYK3* ($n = 11$), *hof1-4E* pGal1-*CYK3* ($n = 7$), *hof1-W637A-GFP* pGal1-*CYK3* ($n = 9$), *hof1-4A-W637A-GFP* pGal1-CYK3 ($n = 9$), *hof1-S533A-S563A-GFP* pGal1-*CYK3* ($n = 10$), *hof1-S533A-S563A-W637A-GFP* pGal1-*CYK3* ($n = 13$), *hof1-S517A-GFP* pGal1-*CYK3* ($n = 12$), *hof1-S517A-W637A-GFP* pGal1-*CYK3* ($n = 6$), and *hof1-S313A-GFP* pGal1-*CYK3* ($n = 7$). Cells were grown in galactose medium (2%) for 24 h at 23°C. At 12 h before inspection, cells were transferred to glucose medium (2%) to repress *CYK3* expression from the Gal1 promoter. (B) Representative kymographs quantified in A. Examples for category C1 (Hof1-GFP), C2 (Hof1-S533A-S563A–GFP Gal1-*CYK3*), and C3 (Hof1-S533A-S563A-W637A–GFP Gal1-*CYK3*). (C) Map showing the statistical significance of differences between the

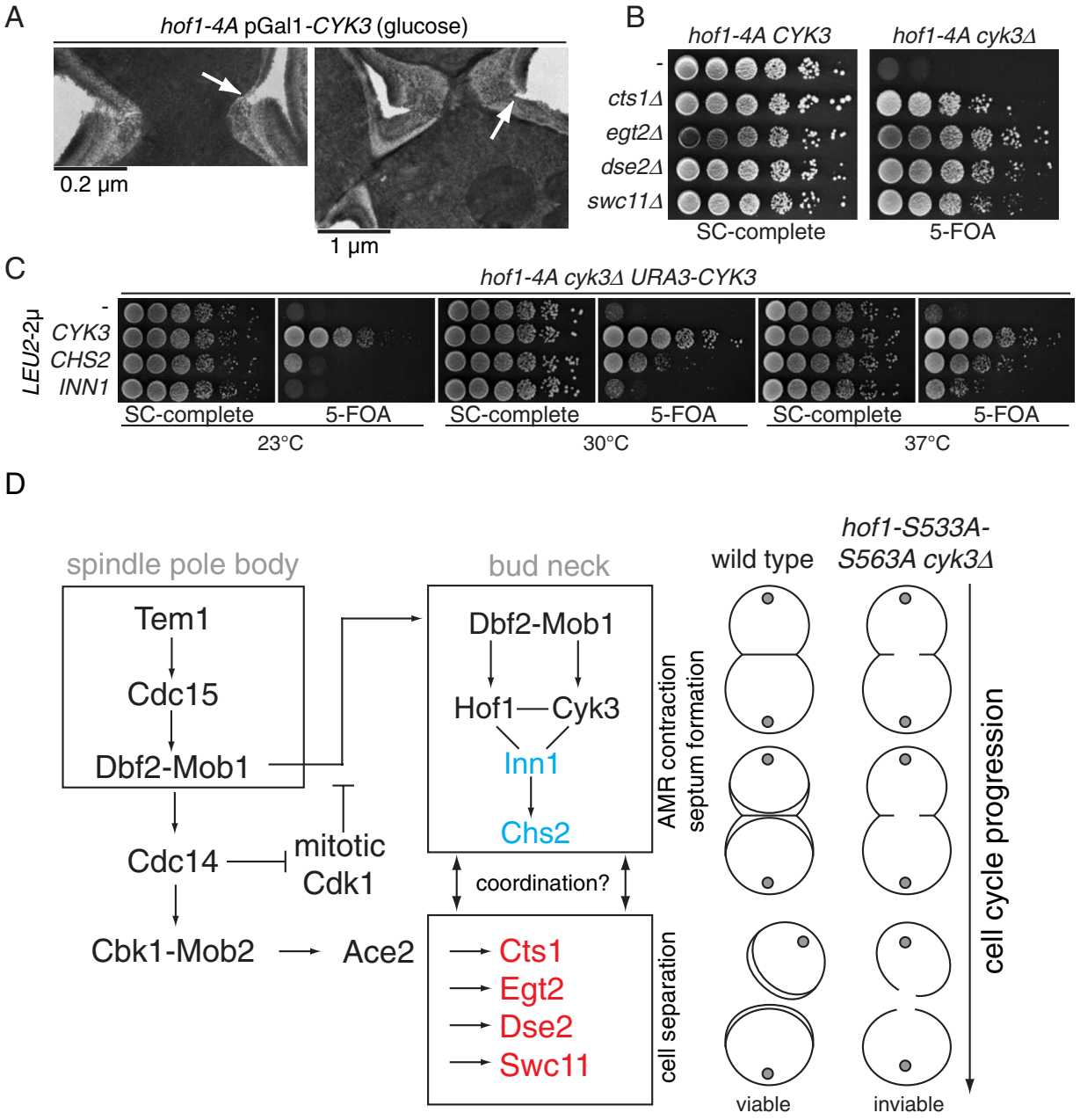

FIGURE 7: Hof1 phosphorylation defects can be bypassed by promoting PS formation or inhibiting PS degradation. (A) TEM images of cross sections of the bud neck region of the *hof1-4A* pGAL-*CYK3* mutant after *CYK3* repression. Arrows indicate the starting process of cell separation. (B) Growth rescue of the *hof1-4A cyk3*Δ mutant after deletion of chitinase or glucanases. (C) Growth rescue of *hof1-4A cyk3*Δ mutant after overexpression of *CHS2* or *INN1*. (D) Model shows pathways controlling cytokinesis and cell separation. Blue proteins can rescue the lethality of *hof1-4A cyk3*Δ and are downstream of Hof1 and Cyk3 in the cytokinesis pathway. Red proteins are important for cell separation and cause lethality in *hof1-4A cyk3*Δ cells.

analyzed mutants (Student's *t* test). (D) The relationship between the duration of Hof1/AMR contraction and cell death. Dead cells were counted after they were grown for 12 h in glucose as described in A. Numbers correspond to the genotypes as shown in A ($n > 100$ per strain). (E) Representative example for cell death during AMR contraction is shown. Left, cell before the onset of cytokinesis (t0), before cell lysis (t44), and after cell lysis (t46). Right, corresponding kymographs for the *x*- and *y*-axes as indicated (t, pictures were taken every 1 min). Scale bar, 5 µm. (F, G) Genetic interactions of indicated genotypes. Cells contain a *URA3*-based plasmid carrying wild-type *CYK3* and were grown in glucose (2%)-containing medium at 23°C. Serial dilutions were spotted onto glucose (2%)-containing plates without or with 5-FOA, which selects against the *URA3*-based plasmid carrying *CYK3*. Plates were incubated at 23°C for 2–3 d. (H) Model for Dbf2-dependent Hof1 regulation during cytokinesis (see the text).

Of interest, the SID locates next to the F-BAR domain that we previously reported to contribute to the recruitment of Hof1 to the bud neck in vivo (Meitinger *et al.*, 2011). This raises the interesting question as to whether the SID and F-BAR domains have interdependent roles in the stabilization of the septin complex. F-BAR domains are known for their membrane-binding ability, which, so far, has not been proven for Hof1. Nevertheless, 3D modeling of the Hof1–F-BAR revealed that positively charged amino acid clusters, which are essential for membrane binding (Frost *et al.*, 2008), are conserved (our unpublished observation). It therefore seems likely that the F-BAR domain of Hof1 binds directly to the membrane. Of interest, the deletion of the F-BAR domain decreases the levels of septin associated with Hof1, which is comparable to the effect of the phosphomimetic Hof1-S313E mutant (Figure 2; Meitinger *et al.*, 2011). In addition, deletion of the FCH domain phenocopies the S313E mutation in being synthetic sick with *SHS1* deletion (our unpublished data). However, the F-BAR domain of Hof1 failed to associate with septins in the yeast two-hybrid system (Figure 1), indicating that the F-BAR domain alone might not be sufficient to mediate the binding to septins. These observations indicate that the F-BAR, together with the SID domain, might have a role in regulating septins in vivo, for example, by connecting septins with the membrane.

Hof1 regulates AMR contraction and septum formation

After mitotic exit, Hof1 moves from septins to the AMR ring, where Hof1 now interacts with Cyk3 and Inn1 proteins to regulate AMR contraction and primary septum formation by an unknown mechanism (Nishihama *et al.*, 2009). Our findings indicate that phosphorylation of C-terminal residues of Hof1 by Dbf2 is the most likely mechanism that facilitates the function of Hof1 in AMR contraction through inhibition of Hof1 protein interaction via its SH3 domain. We previously showed that the phosphoinhibitory *hof1-4A* mutant lacking *CYK3* is unable to survive (Meitinger *et al.*, 2011). A detailed analysis of these cells now shows that the AMR did not contract, remaining in a frozen state that could be reverted through additional inactivation of the SH3 domain (by substitution of tryptophan 637 to alanine; Figure 6; Meitinger *et al.*, 2011). Thus we speculate that a protein with an inhibitory effect on AMR contraction might bind to the SH3 domain of Hof1. One obvious candidate is Cyk3, which is targeted to the bud neck in a Dbf2-dependent manner (i.e., at the same time that Hof1 moves to the AMR ring) and directly interacts with the SH3 domain of Hof1 (Labedzka *et al.*, 2012; Tonikian *et al.*, 2009). One could envisage that the binding of Cyk3 to the SH3 tail of Hof1 could compete with other interacting partners, thereby promoting AMR contraction and/or primary septum formation. However, the inactivation of the PXXP motif of Cyk3, which abrogates its interaction with Hof1 (Labedzka *et al.*, 2012; Tonikian *et al.*, 2009), does not phenocopy *CYK3* deletion in *hof1-4A* cells in respect to cell viability (our unpublished data). Therefore it is unlikely that the frozen AMR in *hof1-4A cyk3*Δ cells result from the missing interaction between Hof1 and Cyk3.

We propose that Dbf2-dependent phosphorylation of Hof1 outside the SID domain might dislodge an inhibitor of AMR contraction that specifically associates with the SH3 domain of Hof1. So far, the identity of this putative inhibitor is unknown. Inn1—one established interaction partner of the SH3 domain of Hof1—might form a stable complex with unphosphorylated Hof1 in the absence of Cyk3. Alternatively, other known interaction partners of the Hof1-SH3 domain, such as Bnr1 and Vrp1, which both regulate actin dynamics, might block AMR contraction (Kamei *et al.*, 1998; Naqvi *et al.*, 2001). However, the inactivation of these proteins by deletion and/or PXXP mutation analysis reverted neither the growth lethality nor AMR contraction of *hof1-4A cyk3*Δ cells (our unpublished data). We therefore anticipate that the identification of Hof1 SH3 interaction partners and their subsequent molecular characterization will constitute important aspects of future research.

Linking cytokinesis with cell separation

Cytokinesis (AMR contraction and septum formation) is followed by cell separation (abscission in mammalian cells), during which daughter and mother cells are physically resolved from one another. How cytokinesis and cell separation are coordinated at the molecular level is not fully understood. The ultrastructural analysis of *hof1-4A cyk3*Δ cells indicated that septum degradation by hydrolases initiates during the process of AMR contraction/primary septum closure. The promotion of primary septum formation via either deletion of septum hydrolases or the ectopic overproduction of Inn1 or Chs2 restored viability to *hof1-4A cyk3*Δ cells, strongly indicating that the onset of cell separation before completion of cytokinesis is deleterious for cell survival. Of interest, in fission yeast the inactivation of the Dbf2 homologue Sid2 leads to a growth lethal phenotype that could be rescued by impairing cell separation (Jin *et al.*, 2006). In budding yeast, both cytokinesis and cell separation are under the control of MEN and Cdc14 (Figure 7D). Activation of Cdc14 by MEN signaling counteracts mitotic Cdk1 function and thereby enables the translocation of Dbf2-Mob1 to the bud neck and the recruitment and activation of Cyk3 and Hof1 (Hwa Lim *et al.*, 2003; Meitinger *et al.*, 2010, 2011). In parallel, Cdc14 activates another NDR kinase, Cbk1, which in turn promotes the function of the transcription factor Ace2 (Brace *et al.*, 2010). Ace2 is responsible for the transcription of septum hydrolases, including chitinase and glucanases. The observation that Cdc14 activates both cytokinesis and cell separation leads to the exciting question as to whether a bud neck–associated mechanism exist that makes the activation of cell separation dependent on the successful completion of cytokinesis. If such a mechanism is in place, it must be inactive in *hof1-4A cyk3*Δ cells, as cell separation starts despite of the incomplete cytokinesis. Thus it is possible that Hof1 and/or Cyk3 are part of such a control mechanism. We therefore anticipate that the identification of the underlying mechanisms by which cell separation/abscission is coordinated with cytokinesis/AMR contraction in a timely manner and the means by which Hof1 and Cyk3 are involved in these processes will provide important insights into the identification of novel cytokinetic control pathways contributing to cell survival.

MATERIALS AND METHODS

Strains, plasmids, growth conditions, and genetic methods

Yeast strains and plasmids used in this study are listed in Supplemental Tables S1 and S2. Yeast growth conditions and media were as described (Sherman, 1991). Gene deletions and epitope tagging were performed using PCR-based methods (Knop *et al.*, 1999; Janke *et al.*, 2004). Yeast strains were grown in yeast/peptone/dextrose medium containing 0.1 mg/l adenine (YPAD). Instead of dextrose, either 3% raffinose (YPAR) or a mixture of 3% raffinose and 2% galactose (YPARG) was used in experiments involving expression of genes under control of the Gal1 promoter. For time-lapse analyses in Figure 6, strains with or without pGal1-*3HA-CYK3* were grown in galactose medium and shifted 12 h before the experiment started into glucose medium to repress *CYK3* expression. Synthetic complete (SC) media lacking corresponding amino acids were used to grow strains carrying plasmids. Loss of *URA3*-containing plasmids was tested using plates containing 1 mg/ml 5-fluoroorotic acid (5-FOA). To test the viability of double mutants, we used a plasmid shuffle strategy. Briefly, mutant strains containing the corresponding wild-type gene on a *URA3*-based plasmid were analyzed for growth on 5-FOA plates (select against *URA3*). At least six individual

transformants were analyzed per double mutant, and one representative mutant is shown. *HOF1-GFP-hphNT1*, *hof1-4A-GFP-hphNT1*, *hof1-4E-GFP-hphNT1*, *hof1-S313E-GFP-hphNT1*, *hof1-S313A-GFP-hphNT1*, *hof1-4A-W637A-GFP-hphNT1*, *hof1-S517A-GFP-hphNT1*, *hof1-S533A-S563A-GFP-hphNT1*, *hof1-S517A-W637A-GFP-hphNT1*, and *hof1-S533A-S563A-W637A-GFP-hphNT1* fragments were cut out from the corresponding plasmids with *Xba*I and *Stu*I and integrated into the genomic *HOF1* locus.

Cell culture synchronization

Cells were synchronized/arrested in metaphase (Figures 1, F and G, and 2, E–G, J, and K) and in anaphase (Figures 2, H–I, and 4). To arrest cells in metaphase, we added 15 µg/ml nocodazole (Sigma-Aldrich, St. Louis, MO) to the culture media and incubated for 2–4 h until >90% of the cells arrested with large buds and one DNA-stained region (4′,6-diamidino-2-phenylindole staining). To provide late-anaphase arrest, 2% galactose was added to the log-phase culture of pGal1-*clb2ΔDB* cells grown in YPAR medium. Alternatively, we arrested cells in late anaphase at 37°C using the temperature-sensitive *dbf2-2 dbf20*Δ double mutant. For the survival test cells were arrested in late anaphase by shifting *dbf2-2 dbf20*Δ cells to 37°C. For the survival test, ~100 cells were plated at time point zero in triplicates on YPD plates. After each hour the same volume was plated as at time point zero. The number of growing colonies gives the number of surviving cells. The survival rate of *hof1-4E* mutant was plotted relative to wild-type cells (Figure 4G). The survival test was repeated twice, with similar outcomes.

Protein detection methods

Yeast protein extracts and Western blotting were performed as described (Janke *et al.*, 2004). Antibodies were rabbit anti-GFP antibody, mouse anti-tubulin (Tub1), mouse anti-HA (clone 12CA5; Sigma-Aldrich), and rabbit anti-Clb2 (Maekawa *et al.*, 2007). Secondary antibodies were goat anti-mouse, goat anti-rabbit, and goat anti-guinea pig immunoglobulins coupled to horseradish peroxidase (Jackson ImmunoResearch Laboratories, West Grove, PA).

Microscopic techniques

For fluorescence still-image analysis, cells carrying GFP or Cherry fusion proteins were fixed in 4% formaldehyde for 10–30 min before inspection. Live-cell imaging and quantification of fluorescence still images were performed as described (Meitinger *et al.*, 2011). Specimens for electron microscopy were prepared as described (Maier *et al.*, 2008).

Protein purifications

Expression of GST, GST-*HOF1-SID* (amino acids [aa] 200–355), GST-*HOF1-SID-S313E* (aa200–355, S313E), GST-*HOF1* (aa521-586), GST-*HOF1* (aa521-586)-*S533A*, and GST-*HOF1* (aa521-586)-*S563A* was induced in *Escherichia coli* BL21 (DE3) at 30°C and purified according to manufacturer's instructions (GE Healthcare, Piscataway, NJ). 6His-Cdc12, Cdc3, Cdc10, and Cdc11 (plasmid pMVB128/133; generous gift from Jeremy Thorner, University of California) were purified as described (Versele and Thorner, 2004). Dbf2-Mob1 was purified from yeast cells as described (Geymonat *et al.*, 2007).

In vitro kinase assay

In vitro kinase assays of purified Dbf2-Mob1 were performed in a kinase reaction buffer containing 50 mM Tris-HCl, pH 7.5, 1 mM dithiothreitol (DTT), 10 mM $MgCl_2$, and 0.1 mM ATP. GST-Hof1 purified from *E. coli* served as substrate. Reactions were held for 30 min at 30°C. We used 5 µCi of γ-[^{32}P]ATP (0.05 nM) per radioactive kinase reaction. Radioactivity was detected using a Bas 1800 II imaging system (Fujifilm, Tokyo, Japan). The detected phosphorylation (P^{32}) was quantified and corrected for background, input of the substrate, and input/activity of Dbf2-Mob1 kinase.

In vitro binding assay

Purified septin complex (6His-Cdc12, Cdc10, Cdc11, and Cdc3) bound to Ni^{2+} nitriloacetic acid agarose beads (Qiagen, Valencia, CA) was washed three times with binding buffer (50 mM Tris-HCl, pH 7.4, 10% glycerol, 100 mM NaCl, 1 mM EDTA, 1 mM DTT, and 0.5% NP-40). Septin complex was mixed with ~2 µg GST, GST-Hof1-CC, and GST-Hof1-CC-S313E and incubated in binding buffer for 1 h at 4°C. The beads were washed eight times with binding buffer and 1% NP-40 and analyzed by SDS–PAGE and Western blotting. Bound GST-Hof1 fragments were calculated as $(I_{\text{Hof1-GST}} - I_{\text{background}})/(I_{\text{septins-6His}} - I_{\text{background}})$, where I is the mean gray value of the protein bands measured using ImageJ (National Institutes of Health, Bethesda, MD).

Immunoprecipitation experiments

For the immunoprecipitation experiment shown in Figure 2B, *dbf2-2 dbf20*Δ *CDC10-TAP* cells carrying *hof1-4E-3HA* or *HOF1-3HA* were arrested for 3h at 37°C. Pellets from a 100-ml yeast culture (10^7 cells/ml) were lysed in a FastPrep FP120 Cell Disturber (MP Biomedicals, Solon, OH) using acid-washed glass beads (Sigma-Aldrich). Lysis buffer contained 50 mM Tris-HCl, pH 7.5, 150 mM NaCl, 10% glycerol, 1 mM EDTA, 1 mM DTT, 350 µg/ml benzamidine, 100 mM β-glycerophosphate, 50 mM NaF, 5 mM $NaVO_3$, and complete EDTA-free protease inhibitor cocktail (Roche, Indianapolis, IN). Cell lysates were incubated with 1% Triton X-100 for 15 min. Total extracts were clarified by centrifugation at 10,000 × *g* for 10 min. Hof1-3HA was immunoprecipitated from total extracts using anti-HA coupled protein A–Sepharose beads (GE Healthcare). Bound Cdc10-TAP was calculated as $(I_{\text{Cdc10-TAP}} - I_{\text{background}})/(I_{\text{Hof1-3HA}} - I_{\text{background}})$, where I is the mean gray value of the protein bands measured using ImageJ.

Yeast two-hybrid assay

Indicated genes or gene fragments were cloned into pMM5 (fusion to LexA) and/or pMM6 (fusion to Gal4) and transformed into the yeast strains YPH500 (*MATalpha*) and SGY37 (*MATa*), respectively. After mating of YPH500 and SGY37 strains the yeast two-hybrid assay was performed as described (Geissler *et al.*, 1996). Interacting proteins activate the expression of β-galactosidase, which converts X-Gal into a blue detectable product.

Amino acid sequence alignment, protein modeling, and coiled-coil prediction

The 3D structure of the Hof1 F-BAR domain was performed by homology-modeling using SWISS-MODEL (Arnold *et al.*, 2006; Kiefer *et al.*, 2009). Protein structures were visualized with the SwissPdb-Viewer (Guex and Peitsch, 1997). Coiled-coil regions were predicted using COILS (Lupas *et al.*, 1991).

ACKNOWLEDGMENTS

We thank Erfei Bi for communicating results before publication; Jeremy Thorner for plasmids; and Elmar Schiebel, Iain Hagan, Fouzia Ahmad, and members of G.P.'s lab for comments on the manuscript. F.M. and S.P. were funded by Marie Curie Grant MEXT-CT-042544. This work was also funded by Helmholtz Young Investigator Grant HZ-NG-111 to G.P. S.P. is funded by the Graduate School Landesgraduiertenförderung, University of Heidelberg, Heidelberg, Germany.

REFERENCES

Arnold K, Bordoli L, Kopp J, Schwede T (2006). The SWISS-MODEL workspace: a web-based environment for protein structure homology modelling. Bioinformatics 22, 195–201.

Aspenstrom P (2009). Roles of F-BAR/PCH proteins in the regulation of membrane dynamics and actin reorganization. Int Rev Cell Mol Biol 272, 1–31.

Balasubramanian MK, Bi E, Glotzer M (2004). Comparative analysis of cytokinesis in budding yeast, fission yeast and animal cells. Curr Biol 14, R806–R818.

Bardin AJ, Amon A (2001). Men and sin: what's the difference? Nat Rev Mol Cell Biol 2, 815–826.

Barr FA, Gruneberg U (2007). Cytokinesis: placing and making the final cut. Cell 131, 847–860.

Blondel M, Bach S, Bamps S, Dobbelaere J, Wiget P, Longaretti C, Barral Y, Meijer L, Peter M (2005). Degradation of Hof1 by SCF(Grr1) is important for actomyosin contraction during cytokinesis in yeast. EMBO J 24, 1440–1452.

Brace J, Hsu J, Weiss EL (2010). Mitotic exit control of the *Saccharomyces cerevisiae* Ndr/LATS kinase Cbk1 regulates daughter cell separation after cytokinesis. Mol Cell Biol 31, 721–735.

Brace J, Hsu J, Weiss EL (2011). Mitotic exit control of the *Saccharomyces cerevisiae* Ndr/LATS kinase Cbk1 regulates daughter cell separation after cytokinesis. Mol Cell Biol 31, 721–735.

Cabib E, Mol PC, Shaw JA, Choi WJ (1993). Biosynthesis of cell wall and septum during yeast growth. Arch Med Res 24, 301–303.

Colman-Lerner A, Chin TE, Brent R (2001). Yeast Cbk1 and Mob2 activate daughter-specific genetic programs to induce asymmetric cell fates. Cell 107, 739–750.

Demeter J, Sazer S (1998). imp2, a new component of the actin ring in the fission yeast *Schizosaccharomyces pombe*. J Cell Biol 143, 415–427.

Dobbelaere J, Gentry MS, Hallberg RL, Barral Y (2003). Phosphorylation-dependent regulation of septin dynamics during the cell cycle. Dev Cell 4, 345–357.

Frenz LM, Lee SE, Fesquet D, Johnston LH (2000). The budding yeast Dbf2 protein kinase localises to the centrosome and moves to the bud neck in late mitosis. J Cell Sci 113, 3399–3408.

Frost A, Perera R, Roux A, Spasov K, Destaing O, Egelman EH, De Camilli P, Unger VM (2008). Structural basis of membrane invagination by F-BAR domains. Cell 132, 807–817.

Geissler S, Pereira G, Spang A, Knop M, Soues S, Kilmartin J, Schiebel E (1996). The spindle pole body component Spc98p interacts with the gamma-tubulin-like Tub4p of *Saccharomyces cerevisiae* at the sites of microtubule attachment. EMBO J 15, 3899–3911.

Geymonat M, Spanos A, Sedgwick SG (2007). A *Saccharomyces cerevisiae* autoselection system for optimised recombinant protein expression. Gene 399, 120–128.

Guex N, Peitsch MC (1997). SWISS-MODEL and the Swiss-PdbViewer: an environment for comparative protein modeling. Electrophoresis 18, 2714–2723.

Holt LJ, Tuch BB, Villen J, Johnson AD, Gygi SP, Morgan DO (2009). Global analysis of Cdk1 substrate phosphorylation sites provides insights into evolution. Science 325, 1682–1686.

Hwa Lim H, Yeong FM, Surana U (2003). Inactivation of mitotic kinase triggers translocation of MEN components to mother-daughter neck in yeast. Mol Biol Cell 14, 4734–4743.

Janke C *et al*. (2004). A versatile toolbox for PCR-based tagging of yeast genes: new fluorescent proteins, more markers and promoter substitution cassettes. Yeast 21, 947–962.

Jin QW, Zhou M, Bimbo A, Balasubramanian MK, McCollum D (2006). A role for the septation initiation network in septum assembly revealed by genetic analysis of sid2–250 suppressors. Genetics 172, 2101–2112.

Kamei T, Tanaka K, Hihara T, Umikawa M, Imamura H, Kikyo M, Ozaki K, Takai Y (1998). Interaction of Bnr1p with a novel Src homology 3 domain-containing Hof1p. Implication in cytokinesis in *Saccharomyces cerevisiae*. J Biol Chem 273, 28341–28345.

Kiefer F, Arnold K, Kunzli M, Bordoli L, Schwede T (2009). The SWISS-MODEL Repository and associated resources. Nucleic Acids Res 37, D387–D392.

Knop M, Siegers K, Pereira G, Zachariae W, Winsor B, Nasmyth K, Schiebel E (1999). Epitope tagging of yeast genes using a PCR-based strategy: more tags and improved practical routines. Yeast 15, 963–972.

Labedzka K, Tian C, Nussbaumer U, Timmermann S, Walther P, Muller J, Johnsson N (2012). Sho1p connects the plasma membrane with proteins of the cytokinesis network through multiple isomeric interaction states. J Cell Sci 125, 4103–4113.

Lippincott J, Li R (1998). Dual function of Cyk2, a cdc15/PSTPIP family protein, in regulating actomyosin ring dynamics and septin distribution. J Cell Biol 143, 1947–1960.

Luca FC, Mody M, Kurischko C, Roof DM, Giddings TH, Winey M (2001). *Saccharomyces cerevisiae* Mob1p is required for cytokinesis and mitotic exit. Mol Cell Biol 21, 6972–6983.

Lupas A, Van Dyke M, Stock J (1991). Predicting coiled coils from protein sequences. Science 252, 1162–1164.

Maekawa H, Priest C, Lechner J, Pereira G, Schiebel E (2007). The yeast centrosome translates the positional information of the anaphase spindle into a cell cycle signal. J Cell Biol 179, 423–436.

Maier P, Rathfelder N, Maeder CI, Colombelli J, Stelzer EH, Knop M (2008). The SpoMBe pathway drives membrane bending necessary for cytokinesis and spore formation in yeast meiosis. EMBO J 27, 2363–2374.

Meitinger F, Boehm ME, Hofmann A, Hub B, Zentgraf H, Lehmann WD, Pereira G (2011). Phosphorylation-dependent regulation of the F-BAR protein Hof1 during cytokinesis. Genes Dev 25, 875–888.

Meitinger F, Palani S, Pereira G (2012). The power of MEN in cytokinesis. Cell Cycle 11, 219–228.

Meitinger F, Petrova B, Lombardi IM, Bertazzi DT, Hub B, Zentgraf H, Pereira G (2010). Targeted localization of Inn1, Cyk3 and Chs2 by the mitotic-exit network regulates cytokinesis in budding yeast. J Cell Sci 123, 1851–1861.

Mortensen EM, McDonald H, Yates J 3rd, Kellogg DR (2002). Cell cycle-dependent assembly of a Gin4-septin complex. Mol Biol Cell 13, 2091–2105.

Naqvi SN, Feng Q, Boulton VJ, Zahn R, Munn AL (2001). Vrp1p functions in both actomyosin ring-dependent and Hof1p-dependent pathways of cytokinesis. Traffic 2, 189–201.

Nishihama R *et al*. (2009). Role of Inn1 and its interactions with Hof1 and Cyk3 in promoting cleavage furrow and septum formation in *S. cerevisiae*. J Cell Biol 185, 995–1012.

Oh Y, Chang KJ, Orlean P, Wloka C, Deshaies R, Bi E (2012). Mitotic exit kinase Dbf2 directly phosphorylates chitin synthase Chs2 to regulate cytokinesis in budding yeast. Mol Biol Cell 23, 2445–2456.

Oh Y, Schreiter J, Nishihama R, Wloka C, Bi E (2013). Targeting and functional mechanisms of the cytokinesis-related F-BAR protein Hof1 during the cell cycle. Mol Biol Cell 24, 1305–1320.

Palani S, Meitinger F, Boehm ME, Lehmann WD, Pereira G (2012). Cdc14-dependent dephosphorylation of Inn1 contributes to Inn1-Cyk3 complex formation. J Cell Sci 125, 3091–3096.

Puig O, Caspary F, Rigaut G, Rutz B, Bouveret E, Bragado-Nilsson E, Wilm M, Seraphin B (2001). The tandem affinity purification (TAP) method: a general procedure of protein complex purification. Methods 24, 218–229.

Ren G, Wang J, Brinkworth R, Winsor B, Kobe B, Munn AL (2005). Verprolin cytokinesis function mediated by the Hof one trap domain. Traffic 6, 575–593.

Schmidt M, Bowers B, Varma A, Roh DH, Cabib E (2002). In budding yeast, contraction of the actomyosin ring and formation of the primary septum at cytokinesis depend on each other. J Cell Sci 115, 293–302.

Sherman F (1991). Getting started with yeast. Methods Enzymol 194, 3–21.

Shimada A *et al*. (2007). Curved EFC/F-BAR-domain dimers are joined end to end into a filament for membrane invagination in endocytosis. Cell 129, 761–772.

Surana U, Amon A, Dowzer C, McGrew J, Byers B, Nasmyth K (1993). Destruction of the CDC28/CLB mitotic kinase is not required for the metaphase to anaphase transition in budding yeast. EMBO J 12, 1969–1978.

Tonikian R *et al*. (2009). Bayesian modeling of the yeast SH3 domain interactome predicts spatiotemporal dynamics of endocytosis proteins. PLoS Biol 7, e1000218.

Tully GH, Nishihama R, Pringle JR, Morgan DO (2009). The anaphase-promoting complex promotes actomyosin-ring disassembly during cytokinesis in yeast. Mol Biol Cell 20, 1201–1212.

Vallen EA, Caviston J, Bi E (2000). Roles of Hof1p, Bni1p, Bnr1p, and myo1p in cytokinesis in *Saccharomyces cerevisiae*. Mol Biol Cell 11, 593–611.

Versele M, Thorner J (2004). Septin collar formation in budding yeast requires GTP binding and direct phosphorylation by the PAK, Cla4. J Cell Biol 164, 701–715.

Versele M, Thorner J (2005). Some assembly required: yeast septins provide the instruction manual. Trends Cell Biol 15, 414–424.

Yang X, Yu K, Hao Y, Li DM, Stewart R, Insogna KL, Xu T (2004). LATS1 tumour suppressor affects cytokinesis by inhibiting LIMK1. Nat Cell Biol 6, 609–617.

Yoshida S, Toh-e A (2001). Regulation of the localization of Dbf2 and mob1 during cell division of *Saccharomyces cerevisiae*. Genes Genet Syst 76, 141–147.

Young BA, Buser C, Drubin DG (2010). Isolation and partial purification of the *Saccharomyces cerevisiae* cytokinetic apparatus. Cytoskeleton (Hoboken) 67, 13–22.